


## Article

# Aristolochic Acid I-Induced Hepatotoxicity in Tianfu Broilers Is Associated with Oxidative-Stress-Mediated Apoptosis and Mitochondrial Damage

Dan Xu <sup>1</sup>, Lizi Yin <sup>2</sup>, Juchun Lin <sup>2</sup>, Hualin Fu <sup>2</sup>, Xi Peng <sup>3</sup>, Lijen Chang <sup>4</sup>, Yilei Zheng <sup>5</sup>, Xiaoling Zhao <sup>1</sup>  and Gang Shu <sup>2,\*</sup>

<sup>1</sup> Farm Animal Genetic Resources Exploration and Innovation Key Laboratory of Sichuan Province, Sichuan Agricultural University, Chengdu 611130, China; 13086605395@163.com (D.X.); zhaoxiaoling@sicau.edu.cn (X.Z.)

<sup>2</sup> Department of Basic Veterinary Medicine, Sichuan Agricultural University, Chengdu 611130, China; yinlizi@hotmail.com (L.Y.); juchunlin@126.com (J.L.); fuhl.sicau@163.com (H.F.)

<sup>3</sup> Sichuan Industrial Institute of Antibiotics, Chengdu University, Chengdu 611130, China; pengxi197313@163.com

<sup>4</sup> Department of Veterinary Clinical Science, College of Veterinary Medicine, Oklahoma State University, Stillwater, OK 74078, USA; lj.chang@okstate.edu

<sup>5</sup> College of Veterinary Medicine, University of Minnesota, Minneapolis, MN 55791, USA; zhen0219@umn.edu

\* Correspondence: dyysg2005@sicau.edu.cn



**Citation:** Xu, D.; Yin, L.; Lin, J.; Fu, H.; Peng, X.; Chang, L.; Zheng, Y.; Zhao, X.; Shu, G. Aristolochic Acid I-Induced Hepatotoxicity in Tianfu Broilers Is Associated with Oxidative-Stress-Mediated Apoptosis and Mitochondrial Damage. *Animals* **2021**, *11*, 3437. <https://doi.org/10.3390/ani1123437>

Received: 26 October 2021

Accepted: 29 November 2021

Published: 2 December 2021

**Publisher's Note:** MDPI stays neutral with regard to jurisdictional claims in published maps and institutional affiliations.



**Copyright:** © 2021 by the authors. Licensee MDPI, Basel, Switzerland. This article is an open access article distributed under the terms and conditions of the Creative Commons Attribution (CC BY) license (<https://creativecommons.org/licenses/by/4.0/>).

**Simple Summary:** Aristolochic acid (AA) is a component of traditional Chinese herbs and commonly used in the farm poultry industry in China for anti-infection, anti-viral and anti-bacterial treatment. However, long-term and over-exposure of these drugs has been proven to be associated with serious hepatotoxicity, but the mechanism of AA-I-induced hepatotoxicity remains unknown. Therefore, in this study, a subchronic toxicity test was conducted to evaluate the mechanism of AA-I-induced hepatotoxicity in Tianfu broilers. Subchronic exposure to high doses of AA-I in broilers can cause serious hepatotoxicity by breaking the redox balance to form oxidative stress, along with promoting oxidative-stress-mediated apoptosis and mitochondrial damage. In conclusion, AA-I has been found to damage broilers' livers in high doses. This study provides suggestions for the clinical application of traditional Chinese medicine containing AA-I in the poultry industry.

**Abstract:** Aristolochic acid (AA) is a component of traditional Chinese herbs and commonly used for farm animals in China. Over-exposure of AA has been proven to be associated with hepatotoxicity; however, the mechanism of action of AA-I-induced hepatotoxicity remains unknown. In the current study, a subchronic toxicity test was conducted to evaluate the mechanism of AA-induced hepatotoxicity in Tianfu broilers. According to the results, AA-I-induced hepatotoxicity in Tianfu broilers was evidenced by the elevation of liver weight, levels of serum glutamic oxalacetic transaminase (GOT) and glutamic-pyruvic transaminase (GPT). Furthermore, hepatocyte swelling, vesicular degeneration and steatosis were observed. Additionally, AA-I elevated the production of reactive oxygen species (ROS) and induced oxidative stress, which further led to excessive apoptosis, characterized by mitochondrial depolarization, upregulation of Bax, and down-regulation of Bcl-2 expression. In conclusion, the mechanism of AA-I-induced hepatotoxicity was associated with oxidative-stress-mediated apoptosis and mitochondrial damage.

**Keywords:** aristolochic acid; liver; oxidative stress; apoptosis; mitochondria

## 1. Introduction

Aristolochic acids (AAs) are chemical components of various natural herbs, especially in Aristolochiaceae [1]. AA exerts various therapeutic effects, including anti-neoplasia, anti-infection, anti-inflammatory, analgesia and anti-fertility [2]. Therefore, AA has been

used extensively for more than 2500 years in many countries as a herbal medication to treat different disease, such as eczema, pneumonia, stroke, hepatitis, snake bites, arthritis and gout [3,4]. AA-I (8-methoxy-3,4-methylenedioxy-10-nitrophenanthrene-1-carboxylic acid, Figure 1) has been recognized as the main toxic component of AA [5], inducing aristolochic acid nephropathy (AAN) [6]. Researchers have indicated that AAN is manifested by rapidly progressive interstitial nephropathy [7], and is thought to occur through multiple mechanisms, such as renal cell apoptosis, renal interstitial inflammatory cell infiltration, oxidative stress and DNA adducts [8,9]. Recently, AA-I-induced DNA adduct accumulation was detected in the liver, which implies that AA-I can induce hepatotoxicity [10,11]. At the same time, many reports have evidenced the direct association between the use of AA and hepatitis-B-related liver cancer [12]. Although the renal toxicity of AA-I has been clearly documented to date, information regarding AA-I-induced hepatotoxicity remains scant and unclear. The liver plays an important role in drug and toxin metabolism [13]; thus, the mechanism of action of AA-I-induced liver injury should be identified.

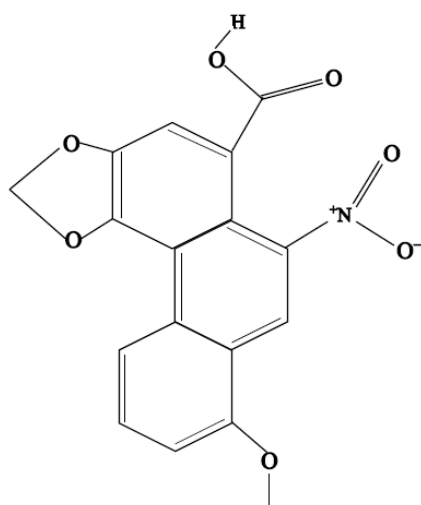


**Figure 1.** Chemical structure of aristolochic acid A.

The use of botanical drugs containing AA has been prohibited in many countries due to its toxic effects [14]. However, there are three drugs derived from the *Aristolochia* family, including *Aristolochia*, *Herba Aristolochiae*, and *Asarum heterotropoides* that remain in the Pharmacopoeia of PR China for clinical use to date as complementary remedies for poultry husbandry, especially used as a feed additive in domestic poultry, leading to a potential hazard to domestic poultry husbandry [15]. Moreover, a recent study also indicated that AA-I could move from *Aristolochia* family herbs to other plant species via a common matrix: the soil, which may make it easier for animals to be exposed to AA-I [16]. Therefore, it is necessary to recognize the toxicity of AA-I systemically, thus providing appropriate guidance regarding the clinical use of AA-I.

Exogenous chemicals can be metabolized to active metabolites by hepatic enzymes in the liver, which may further induce free radicals and lead to peroxidation. Hepatocyte apoptosis and necrosis can be triggered by the aforementioned active metabolites, leading to hepatic injury and hepatic carcinogenesis [17]. Moreover, most of the complications associated with hepatic injury are mediated by oxidative stress, oxidative-stress-related mediators and inflammation [18]. It has been indicated that oxidative stress, apoptosis and inflammation play important roles in AA-induced toxicity [19–21].

The LD<sub>50</sub> of AA-I to induce subchronic toxicity in Tianfu broilers has been determined in a previous study [15]. The aim of this study is to explore the mechanism of AA-I-induced hepatotoxicity, including oxidative stress, oxidative-stress-mediated apoptosis and mitochondrial damage, in order to provide guidance for the application of AA-I in domestic poultry husbandry.

## 2. Material and Methods

### 2.1. Experimental Materials

Aristolochic acid A (AA, HPLC > 98%) was purchased from Chengdu Rifens Technology Co., Ltd., Sichuan, China. TRIzol reagent (Nanjing Jiancheng Bioengineering Institute, Nanjing, China), total ROS assay kit (Thermo Fisher, Waltham, MA, USA), MMP detection JC-1 kit (BD Bioscience, Franklin Lakes, NJ, USA), eBioscience™ Annexin V-FITC Apoptosis Kit (Invitrogen, Shanghai, China), and reverse transcription reagents (TaKaRa, Kyoto, Japan) were purchased from the relevant companies. The chicken-specific ELISA assay kits for glutamic oxalacetic transaminase (GOT), glutamic-pyruvic transaminase (GPT), total antioxidant capacity (T-AOC), malondialdehyde (MDA), superoxidase dismutase (SOD) and glutathione (GSH) were purchased from Nanjing Jiancheng Bioengineering Institute (Nanjing, China).

### 2.2. Experimental Animals

The study has been approved by the Institutional Animal Care and Use Committee of Sichuan Agricultural University (permission number DYY-2018203007) and was conducted at the poultry farm of Sichuan Agricultural University. Animals and procedures were conducted in accordance with the regulations of the national standard Laboratory Animal Requirements of Environment and Housing Facilities (GB 14925–2001).

Forty, 1-day-old, male Tianfu broilers with body weight of  $38.83 \pm 3.45$  g from the Poultry Breeding Farm of Sichuan Agricultural University (Sichuan, China) were used in this study. All subjects were captive in a climate-controlled facility with air-ventilator and the relative humidity was kept at 50%. The photoperiod was maintained at 24 h for the first 14 days, followed by 20 h for the rest of the study. The temperature was set at 34 °C initially, followed by decremented 2 °C per week until the temperature reached 26 °C, which was maintained throughout the study. Food and water were free to access throughout the study. The daily diet formulation was determined according to the National Research Council requirements for chickens (Supplementary Table S1) [22].

### 2.3. Subchronic Poisoning with Aristolochic Acid A in Tianfu Broilers

Three different doses (1/100, 1/50, and 1/10) of LD50, with these amounts determined in a previous study [15], were used to induce 28-day subchronic toxicity tests in broilers to evaluate the mechanism of AA-I-induced biochemical profile and liver histopathological changes.

Forty, 1-day-old, male broilers were randomly divided into four groups. Subjects in the control group (CG) received normal saline. AA-I at 1/100, 1/50, and 1/10 of LD50 was administered to subjects in the low-dose group (LAG), middle-dose group (MAG), and high-dose group (HAG), respectively. Drugs were administered intraperitoneally in all groups. Subjects were acclimated in the facility for 24 h (D 0), followed by the administration of experimental agents once daily (q 24 h) for 28 days (D 1 to D 28).

#### 2.3.1. Sample Collection and Liver Cell Separation

All subjects were sacrificed, and samples were collected on D 29. The liver was weighed and the ratio of liver weight to body weight (g/kg) (relative liver index) was calculated.

Liver samples were fixed in 4% (*w/v*) buffered paraformaldehyde for histology. The remaining liver samples were flushed by 0.9% normal saline for biochemical analysis. The harvested hepatic cells were used for flow cytometry analysis. The method of harvesting hepatic cells has been described elsewhere [17].

#### 2.3.2. Biochemical Analysis

The levels of serum GOT, serum GPT, and hepatic MDA, GSH, T-AOC and SOD were detected by specific ELISA kits. The method of biochemical analysis has been described in a previous study [23].

### 2.3.3. Histopathology

The method for detection of histological changes has been described in a previous study [24]. The fixed samples were dehydrated, cleaned, embedded in paraffin, and sliced to 5  $\mu\text{m}$  slices by use of an RM2235 microtome (Leica, Munich, Germany). Sliced samples were flattened and dried on glass slides, stained with hematoxylin and eosin (Thermo, Waltham, MA, USA), and sealed with neutral resin. The histopathological changes were observed by a CX22 microscope (Olympus, Tokyo Metropolitan, Japan) and a DM1000 microimaging system (Leica, Munich, Germany) was applied for image recording. In pathological diagnosis, we used INHAND criteria (Table 1) to judge the severity of histological lesions [25].

**Table 1.** Illustration of a 4-point scoring system.

Numerical Score	Description	Definition
0	Within normal limits	Tissue considered to be normal, under the conditions of the study and considering the age, sex, and strain of the animal concerned. Alterations may be present, which, under other circumstances, would be considered deviations from normal.
1	Minimal	The amount of change present barely exceeds that which is considered to be within normal limits.
2	Slight	In general, the lesion is easily identified but of limited severity.
3	Moderate	The lesion is prominent, but there is significant potential for increased severity.
4	Severe	The degree of change is as complete as possible (occupies the majority of the organ).

### 2.3.4. Reactive Oxygen Species (ROS), Mitochondrial Membrane Potential (MMP) and Apoptosis by Flow Cytometry

The prepared hepatocytes were incubated with DCFH-DA (total ROS assay kit), JC-1, and 5  $\mu\text{L}$  of Annexin V-FITC and 5  $\mu\text{L}$  of PI, respectively. All hepatocytes were incubated in a dark environment at 37  $^{\circ}\text{C}$  for 15 min. A cytometry flowmeter (Bio-Rad, Hercules, CA, USA) was used to detect reactive oxygen species (ROS, %), mitochondrial membrane potentials (MMPs) and the percentage of apoptosis. The MMP result was described as a mitochondrial depolarization ratio. All aforementioned data were translated and recorded by Kaluza 2.1 Software, Beckman Coulter, CA, USA.

### 2.3.5. Ultrastructure Observations

The observation criteria of ultrastructure were published elsewhere [26]. Liver samples were sliced and fixed in 2.5% glutaraldehyde (pH = 7.4) at 4  $^{\circ}\text{C}$ , followed by osmium tetroxide ( $\text{OsO}_4$ ) for post-fixation. The samples were soaked and embedded in epoxy resin acetone solution once dried. The samples were sliced to 80 nm slices by Microtome. Samples were stained by lead citrate and uranyl acetate solutions. Ultrastructure of ileum was observed by an HT7700 transmission electron microscope (Hitachi, Tokyo, Japan) and photographs were taken by a GANTAN830.10W CCD camera (Hitachi, Tokyo, Japan). In pathological diagnosis, we used INHAND criteria (Table 1) to judge the severity of histological lesions [25].

### 2.3.6. Fluorescence Real-Time Quantification PCR (QRT-PCR)

Samples were rinsed by pre-frozen Diethylpyrocarbonate (DEPC) water and then frozen in liquid nitrogen at  $-80^{\circ}\text{C}$ . Approximately 60 mg of frozen sample was ground thoroughly in a precooling tissue homogenizer. Total RNA was extracted by a commercial kit (TRIzol, Invitrogen, Shanghai, China). The RNA concentration was detected by a nucleic acid protein analyzer which had the D260/D280 reverse transcription eligible range at 1.8–2.0. The cDNA was stored at  $-80^{\circ}\text{C}$ .

According to the operator's manual, QRT-PCR could be used to detect the expression of Nrf2, NQO1, HO-1, Bax and Bcl-2, and  $\beta$ -actin could be used for normalizing the expression of aforementioned genes as an endogenous control. In this study, the expression of the aforementioned genes in CG was defined as baseline (value = 1), and the  $2^{-\Delta\Delta\text{Ct}}$  method

was applied for quantifying gene expressions, where  $\Delta\Delta Ct$  is the detected  $\Delta Ct$ - reference  $\Delta Ct$  and  $\Delta Ct$  is the  $Ct_{\text{target gene}} - Ct_{\text{housekeeping gene}}$ . Primers used in the present study (Supplementary Table S2) were designed by Premier 5 (PREMIER Biosoft International, New York, NY, USA) and synthesized by Chengke BioTech Co., Ltd. (Guangzhou, China).

#### 2.4. Statistical Analyses

All parameters were presented as mean  $\pm$  standard error (mean  $\pm$  SE) in this study. Duncan's test was used to determine the differences among treatment groups. Data were analyzed by one-way analysis of variance (ANOVA) with SPSS 19.0 (SPSS Inc., Chicago, IL, USA). Significance was determined when  $p < 0.05$ .

### 3. Results

#### 3.1. AA-I Elevated Liver Index in Broilers

The macroscopic characteristics of liver samples are shown in Figure 2A. Samples in CG were normal under gross inspection with red-brown, bright and damp surfaces, whereas samples in treatment groups, especially in MAG and HAG, showed swollen, firm, fragile grossly and diffused yellowish-brown steatosis lesions. Compared with the CG, the liver index in MAG and HAG increased significantly ( $p < 0.05$ ) after intraperitoneal administration of AA-I for 28 days. The liver index results are shown in Figure 2B.

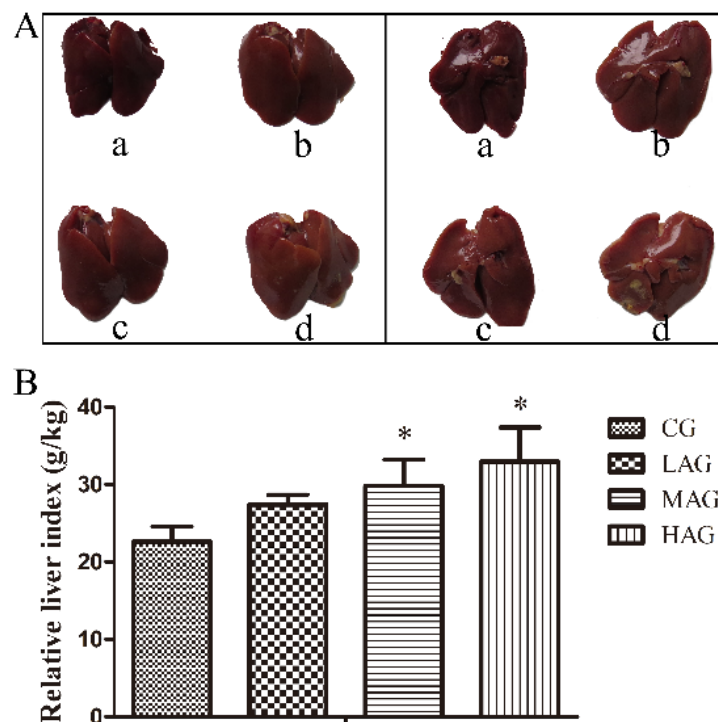


**Figure 2.** (A): Liver morphology in different groups. a: CG group, b: LAG group, c: MAG group, d: HAG group. (B): Liver index of broilers in different groups. \*  $p < 0.05$ , compared with the control group (CG).

#### 3.2. AA-I Elevated Hepatic Enzymes in Broilers

The serum transaminase levels are shown in Figure 3. Compared with the CG, all AA-I treatment groups recorded significant higher levels of serum GOT ( $p < 0.05$ ), and nearly doubled levels were observed in MAG and HAG ( $p < 0.05$ ). For serum GPT, both MAG and HAG showed significant elevations of serum GPT in comparison with that of CG ( $p < 0.05$ ).

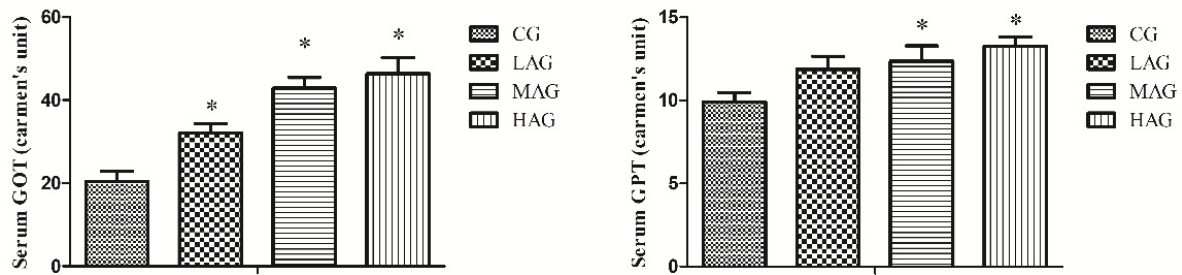


**Figure 3.** Effects of aristolochic acid A on the liver function of Tianfu broilers. \*  $p < 0.05$ , compared with the control group (CG). GOT: glutamic oxalacetic transaminase ( $\mu\text{mol/L}$ ), GPT: glutamic-pyruvic transaminase ( $\text{mmol/L}$ ).

### 3.3. AA-I Deformed Hepatocyte Structures

The results of the histopathological changes of hepatocytes are shown in Figure 4. Hepatocytes in CG were normal in structure and cellular arrangements. AA-I-induced hepatocyte degeneration and necrosis in all intervention groups presented in a dose-dependent manner. Adipose changes and the cloudy swelling of hepatocytes were recognized by observations of red granular substances, irregular or circular vacuoles in the cytoplasm. Necrotic hepatocytes could be identified by pyknosis, karyorrhesis, and karyolysis. In LAG, mild hepatocyte degeneration and mild narrowing of hepatic sinuses were observed. In the MAG, moderate histopathological lesions of the liver were recognized by adipose degeneration, hydropic degeneration and the disappearance of hepatic sinuses. The severest lesions were found in the HAG, where hepatocytes showed severe swelling, vesicular degeneration and steatosis. Furthermore, mild congestion with a large number of hepatic sinuses narrowed and/or disappeared were observed.

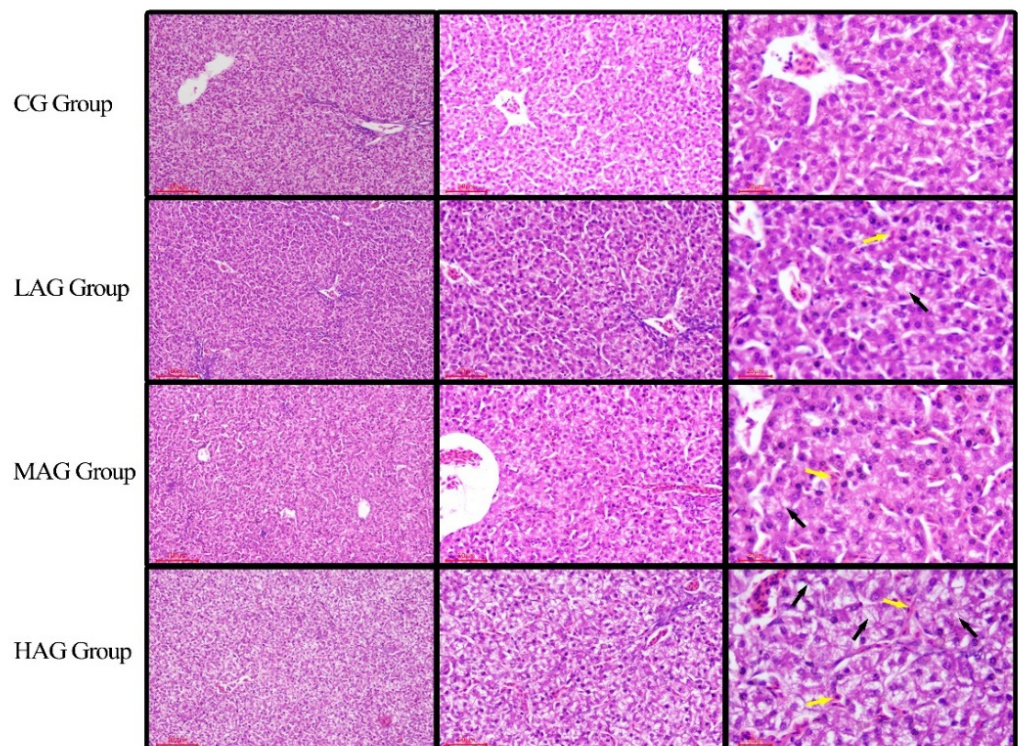


**Figure 4.** The histopathological changes of hepatocytes induced by AA-I in Tianfu broilers. H.E. stain, the left magnification:  $100\ \mu\text{m}$ , the medium magnification:  $50\ \mu\text{m}$ , the right magnification:  $20\ \mu\text{m}$ . Yellow arrows: red blood cells; black arrows: hepatocyte vesicular degeneration.

### 3.4. AA-I Impacted Antioxidant System and Aroused Oxidative Stress

SOD levels decreased significantly in all treatment groups in comparison with the CG ( $p < 0.05$ ). Both GSH and T-AOC in the HAG showed significant decreases when compared to the CG ( $p < 0.05$ ), whereas compared with the CG, the results revealed that AA-I-induced MDA and ROS accumulation in the liver is due to the significant elevation of MDA and ROS levels in the HAG ( $p < 0.05$ ). All results are shown in Figure 5.

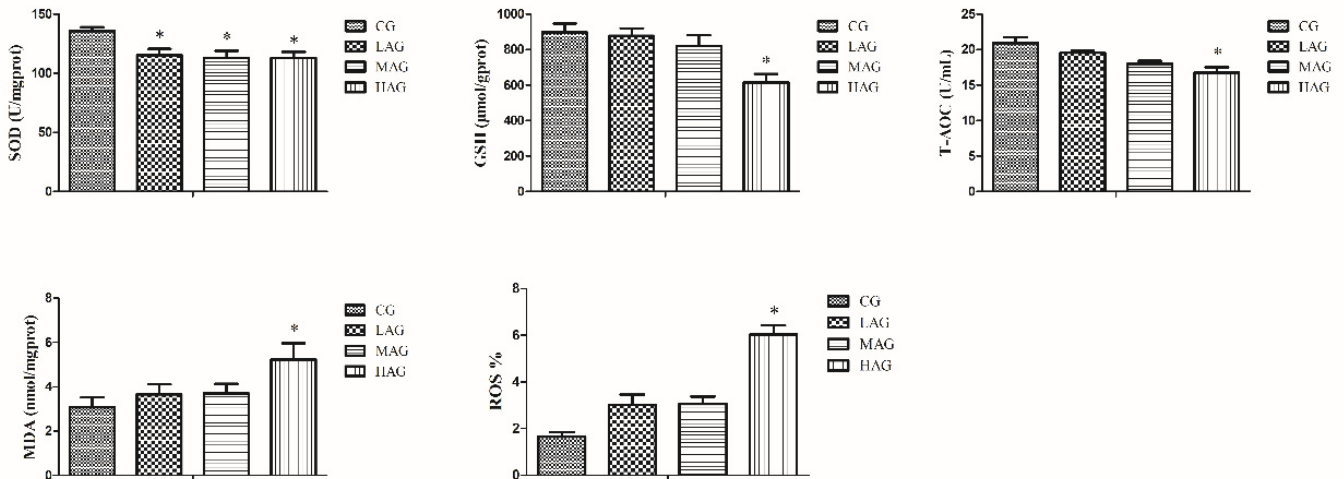


**Figure 5.** Effects of aristolochic acid A on the antioxidant system of Tianfu broiler. \*  $p < 0.05$ , compared with the control group (CG). MDA: malondialdehyde (mmol/L), SOD: superoxidase dismutase (U/mL), GSH: glutathione ( $\mu\text{mol/g}$ ), and T-AOC: total antioxidant capacity (U/mL); ROS: reactive oxygen species (%).

Furthermore, the relative mRNA levels of antioxidant stress genes were evaluated in the present study. According to the results of QRT-PCR (Figure 6), compared with the CG, the expression of Nrf2, NQO1 and HO-1 mRNA were significantly lower in the MAG and HAG ( $p < 0.05$ ).

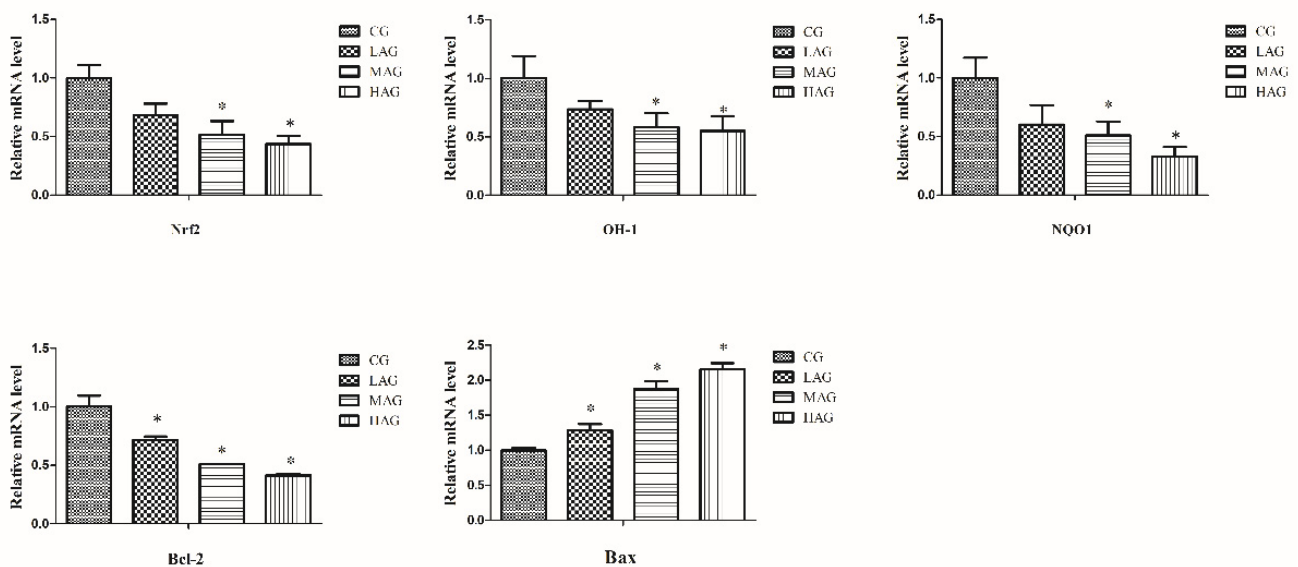


**Figure 6.** The mRNA expression of genes (NQO1, HO-1, Nrf2, Bax, and Bcl-2) of liver in each group. \*  $p < 0.05$ , compared with the control group (CG).

### 3.5. AA-I Induced Mitochondrial Damage and Apoptosis in Hepatocytes

The results of mitochondrial damage and hepatocytes apoptosis are shown in Figure 7. The proportions of mitochondrial depolarization were significantly elevated in the HAG as compared with the CG ( $p < 0.05$ ). Compared with the CG, the percentage of hepatocytes apoptosis was significantly elevated in all AA-I treatment groups ( $p < 0.05$ ).

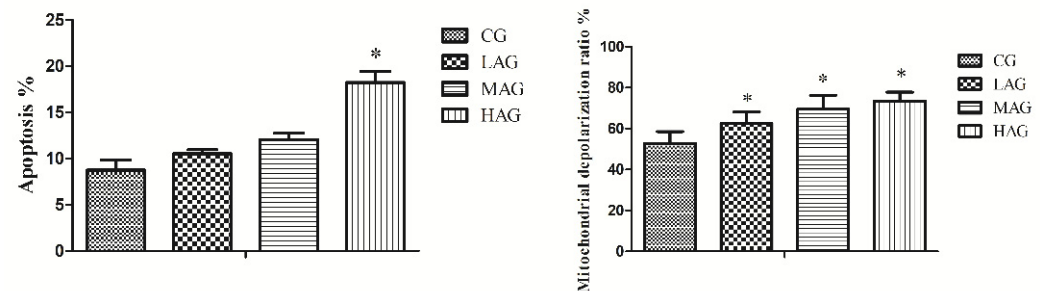


**Figure 7.** The mRNA expression of genes (NQO1, HO-1, Nrf2, Bax, and Bcl-2) of livers in each group. \*  $p < 0.05$ , compared with the control group (CG).

The ultrastructure of hepatocytes is presented in Figure 8. The ultrastructure of hepatocytes in the CG (Figure 8A) appeared normal, with complete mitochondria which have a clear membrane and aligned bridges, intact endoplasmic reticulum, and normal distribution of glycogen particles. The ultrastructure of hepatocytes in the LAG showed swollen mitochondria with decreased electron density in the cytoplasm, and local glycogen particles gathered together (Figure 8B). In the MAG, the electron density in mitochondria was lower and more severe mitochondrial structure pathological changes were observed. Furthermore, hepatocyte apoptosis with concentrated and marginated chromatin was also noticed (Figure 8C,D). It was also noticed that hepatocytes in the MAG showed an indistinct internal structure of cytoplasm, in which large numbers of lysosomes, and glycogen aggregation could be found. In addition, some fuzzy internal structural lumpiness with low electron density, which contained some suspected glycogen and membrane components, were seen. It was observed that the histological changes of hepatocytes in the HAG were similar to those in the MAG. However, the degree of cellular ultrastructure changes was severer than that in the MAG (Figure 8E–H). Furthermore, the hepatocytes in the HAG showed the following histopathological changes: (1) expansion of the mitochondrial outer membrane, (2) cellular vacancy, (3) aggregation of large numbers of secondary lysosomes with uneven electron density, (4) locally, some double-layer membrane circular cavity which contained striated structural materials was present in the liver cytoplasm.

The relative mRNA levels of apoptotic genes involved in the mitochondrial apoptotic pathway were also measured in the present study. As shown in Figure 6, compared with the CG, the mRNA expression of Bcl-2 was apparently down-regulated among all AA-I treatment groups ( $p < 0.05$ ). Additionally, the mRNA expression of Bax increased significantly in all AA-I treatments relative to the control ( $p < 0.05$ ).



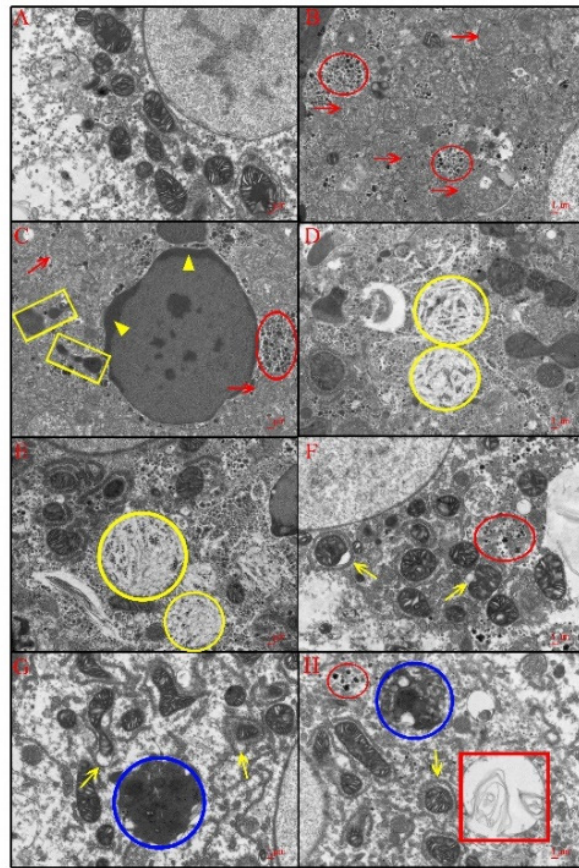


**Figure 8.** Ultrastructure observations of livers in different groups. (A): CG group; (B): LAG group; (C,D): MAG group; (E–H): HAG group; scale bar = 10  $\mu$ m. Red circle: glycogen aggregation; yellow circle: fuzzy internal structural lumpiness with low electron density; blue circle: secondary lysosomes with uneven electron density; yellow triangle: the chromatin concentrated and shifted in the nucleus; red arrow: swollen mitochondria; yellow arrow: the mitochondria outer membrane expanded, locally forming a vacancy; red box: double-layer membrane circular cavity containing striated structure material; yellow box: the number of lysosomes increased significantly.

#### 4. Discussion

Aristolochic acids (AAs) are chemical components which are abundant in traditional Chinese medicines, which have been used commonly as an alternative to antibiotics in the poultry and livestock industries due to the variety of therapeutic effects [27]. However, excessive exposure to AA, especially AA-I, may induce undesired adverse effects [14]. At present, AA-I toxicity has been noticed extensively. It has been proven that the long-term administration of AA-I can be carcinogenic and nephrotoxic in rats, mice, rabbits, pigs and humans [28–30]. However, there is scant information regarding the detrimental effects and mechanism of AA-I-induced poultry hepatotoxicity. The present study results reveal that a high dosage of AA-I induces severe hepatotoxicity due to oxidative stress injury, mitochondrial damage and apoptosis of the hepatocytes in Tianfu broilers, which leads to irreversible hepatic dysfunction.

The liver plays an important role of various biological activities, including bile acid secretion, immunization, detoxification and metabolism [31]. It has been reported that histopathological alterations of the liver can be triggered by exposure to microorganisms, metals, drugs, and so on, and result in liver dysfunction [32]. In this study, the results indicated that AA-I can trigger histopathological lesions of hepatocytes in a dose-dependent manner. It has been proven that hepatic parenchyma injury can be recognized by elevation of the liver index [33]. In the present study, elevation of the liver index among all treatment

groups can be evidence of liver injury. The levels of serum GOT and GPT are two important indicators of liver function, and the abnormally high levels are generally tested as predictors of liver dysfunction [34,35]. Nevertheless, the significant elevation of serum GOT and GPT levels revealed the true AA-I-induced hepatotoxicity in Tianfu broilers. Overall, the present results indicate that AA-I can cause an increase in the liver index and the elevation of serum GOT and GPT, which is in accordance with the results from Yeh et al.'s study in 2008 [36]. It has been reported that AA-I can induce diffuse hepatocyte swelling and vacuolar degeneration in rats [37]. Similarly, the current result of histopathological changes indicated that AA-I caused hepatocyte injury in a dose-dependent manner and the histopathological changes are characterized by obvious hepatocyte swelling, vesicular degeneration and steatosis.

Although the hepatotoxicity of AA-I has been widely presented in several works, the comprehension of its underlying mechanism remains unknown. It has been indicated that oxidative stress plays an essential role in AA-I-induced liver damage [10,38]. Oxidative stress disrupts the oxidation–reduction balance, which is commonly seen in many biological reactions with increases in ROS levels [39]. The results of this study show that AA-I promoted the accumulation of ROS and MDA, and the suppression of SOD, T-AOC and GSH performance, indicating that continuous exposure to an overdose of AA-I breaks down the redox homeostasis and induces oxidative stress in the hepatocytes of Tianfu broilers. It has been reported that AA-N induces endothelial cell toxicity by the elevation of intracellular ROS levels and inhibition of cellular antioxidant function [40]. Additionally, Zhang et al. [41] indicated that exposure to AA-I perturbed the progression of oocyte meiotic and fertilization capacity by the induction of excessive oxidative stress, which led to DNA damage and apoptosis. It has also been proven that AA-I can induce significant downregulation of the Nrf2-HO-1/NQO1 pathway, an efficient antioxidant, and lead to oxidative stress [42,43].

Oxidative stress is a crucial factor for the induction of apoptosis and excessive ROS promotes cell degradation and death [44]. Romanov et al. [45] reported that a high dose of AA induced renal cell apoptosis by increasing the production of ROS. In the present study, the apoptosis rate of hepatocytes increased significantly in all treatment groups. In order to specify the mechanism of AA-I-induced apoptosis, the biomarkers were strictly limited to the Bcl-2 family (Bcl-2 and Bax) [46]. In the present study, AA-I increased the mRNA expression of Bax, whereas it decreased the expression of Bcl-2. Moreover, it has been reported that the imbalance of the Bax and Bcl-2 ratio and the elevation of mitochondrial depolarization can initiate a mitochondrial apoptotic pathway [47]. Therefore, the significant increase in mitochondrial depolarization in this study implies that AA-I can activate the mitochondria-regulated apoptotic signal transduction. Furthermore, the findings of hepatocyte ultrastructure changes also prove the occurrence of cellular apoptosis. It has been revealed in several studies that AA-I-induced ROS accumulation can cause the disruption of mitochondria. The mitochondria became swollen with decreased electron density and the mitochondrial transmembrane potentially collapses, leading to mitochondrial dysfunction [48]. Furthermore, numerous electrons leaked out from the uncoupled electron transport chain following the process of uncoupled oxidative phosphorylation in energy respiration, thereby resulting in large amounts of ROS generation, and further arousing explosive oxidative stress [49,50]. Liu et al. [51] have proven that mitochondrial dysfunction is involved in AA-I-induced apoptosis in renal proximal tubular epithelial cells. Nevertheless, the disorder of mitochondrial microstructure and function are associated with AA-I-induced hepatocyte apoptosis and oxidative damage.

## 5. Conclusions

To conclude (as summarized in Figure 9), the current work demonstrates that AA-I induced hepatotoxicity after subchronic exposure in Tianfu broilers in a dose-dependent manner. It breaks the redox balance of the liver, which further triggers oxidative-stress-mediated apoptosis and mitochondrial damage, eventually leading to liver damage.

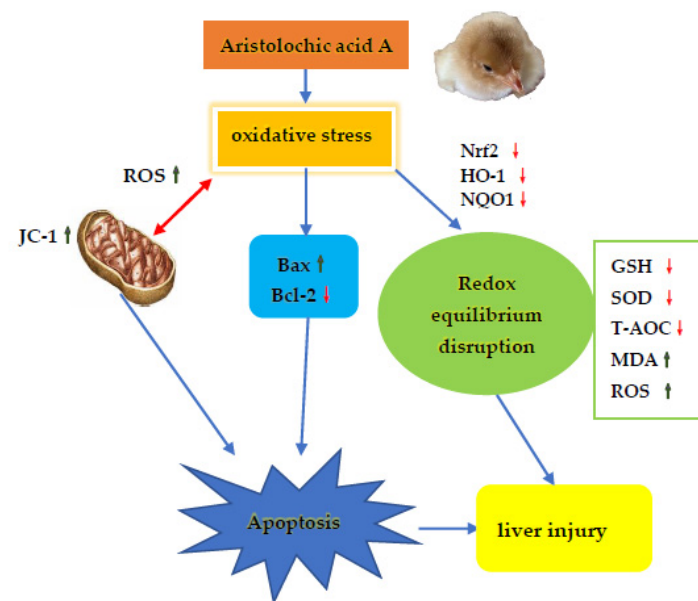


**Figure 9.** Schematic diagram of the possible mechanism of AA-I-induced liver injury in Tianfu broilers. The toxicological mechanism of AA-I-induced liver injury contains excessive apoptosis and oxidative stress damage.

**Supplementary Materials:** The following are available online at <https://www.mdpi.com/article/10.3390/ani11123437/s1>, Supplementary Table S1. Composition and nutrient levels of the basal diet (air-dry basis) (g/kg). Supplementary Table S2. Primer information for qRT-PCR assays. Supplementary Figure S1. The flow cytometry quadrant diagrams of ROS levels in liver. A: CG group, B: LAG group, C: MAG group, D: HAG group. Supplementary Figure S2. The flow cytometry quadrant diagrams of apoptosis in liver. A: CG group, B: LAG group, C: MAG group, D: HAG group. Supplementary Figure S3. The flow cytometry quadrant diagrams of mitochondrial depolarization ratio in liver. A: CG group, B: LAG group, C: MAG group, D: HAG group.

**Author Contributions:** Study and experiments were conceived and designed by D.X. and G.S. Bird raising, reagent preparation, sample collection, and data analysis were performed by L.Y. and J.L. Data analysis and interpretation were performed by X.P., X.Z. and H.F. The manuscript was written and prepared by D.X., Y.Z. and L.C. Assessment of macro, micro and ultrascopic liver/hepatocytes morphology were performed by X.P. and L.C. All authors have read and agreed to the published version of the manuscript.

**Funding:** This work was supported by grants from the National Foundation of Natural Science of China (31872347).

**Institutional Review Board Statement:** The study was approved by the Institutional Animal Care and Use Review Board of the Sichuan Agricultural University under permit number DYY-2018203007, 2020. For all broilers, best clinical practice in respecting patient health was guaranteed for every animal in accordance with the national standard Laboratory Animal Requirements of Environment and Housing Facilities (GB 14925–2001).

**Informed Consent Statement:** Not applicable.

**Data Availability Statement:** The data presented in this study are available on request from the corresponding authors. The data are not publicly available due to privacy protection.

**Acknowledgments:** The authors would like to thank Zheng-Qiang Yu and Jiajia Deng from Yankester Biotechnology Co., Ltd., Chengdu, Sichuan, China for insightful comments on the assessment of macro, micro and ultrascopic liver/hepatocytes morphology.

**Conflicts of Interest:** The authors declare no conflict of interest.

## References

1. Yang, H.Y.; Chen, P.C.; Wang, J.D. Chinese Herbs Containing Aristolochic Acid Associated with Renal Failure and Urothelial Carcinoma: A Review from Epidemiologic Observations to Causal Inference. *BioMed. Res. Int.* **2014**, *2014*, 569325. [[CrossRef](#)] [[PubMed](#)]
2. Anandagoda, N.; Lord, G.M. Preventing Aristolochic Acid Nephropathy. *Clin. J. Am. Soc. Nephro.* **2015**, *10*, 167–168. [[CrossRef](#)] [[PubMed](#)]
3. Vanherweghem, J.; Depierreux, M.; Tielemans, C.; Abramowicz, D.; Vanhaelen-Fastre, R. Rapidly progressive interstitial renal fibrosis in young women: Association with slimming regimen including Chinese herbs. *Lancet* **1993**, *341*, 387–391. [[CrossRef](#)]
4. Abdullah, R.; Diaz, L.N.; Wesseling, S.; Rietjens, I. Risk assessment of plant food supplements and other herbal products containing aristolochic acids using the margin of exposure (MOE) approach. *Food Addit. Contam.* **2017**, *34*, 135–144. [[CrossRef](#)] [[PubMed](#)]
5. Shibutani, S.; Dong, H.; Suzuki, N.; Ueda, S.; Miller, F.; Grollman, A.P. Selective Toxicity of Aristolochic Acids I and II. *Drug Metab. Dispos.* **2007**, *35*, 1217–1222. [[CrossRef](#)] [[PubMed](#)]
6. Chang, S.Y.; Weber, E.J.; Sidorenko, V.S.; Chapron, A.; Yeung, C.K.; Gao, C.Y.; Mao, Q.C.; Shen, D.; Wang, J.; Rosenquist, T.A. Human liver-kidney model elucidates the mechanisms of aristolochic acid nephrotoxicity. *JCI Insight* **2017**, *2*, e95978. [[CrossRef](#)] [[PubMed](#)]
7. Wang, Z.H.; He, B.S.; Liu, Y.Q.; Huo, M.L.; Fu, W.Q.; Yang, C.Y.; Wei, J.F.; Abliz, Z. In situ metabolomics in nephrotoxicity of aristolochic acids based on air flow-assisted desorption electrospray ionization mass spectrometry imaging. *Acta. Pharm. Sin. B* **2020**, *10*, 1083–1093. [[CrossRef](#)] [[PubMed](#)]
8. Yang, Y.J.; Geng, X.D.; Chi, K.; Liu, C.; Liu, R.; Chen, X.M.; Hong, Q.; Cai, G.Y. Ultrasound enhances the therapeutic potential of mesenchymal stem cells wrapped in greater omentum for aristolochic acid nephropathy. *Stem. Cell Res. Ther.* **2021**, *12*, 1–16. [[CrossRef](#)]
9. Prabu, S.M.; Muthumani, M. Silibinin ameliorates arsenic induced nephrotoxicity by abrogation of oxidative stress, inflammation and apoptosis in rats. *Mol. Biol. Rep.* **2012**, *39*, 11201–11216. [[CrossRef](#)] [[PubMed](#)]
10. Marin, D.E.; Pistol, G.C.; Gras, M.; Palade, M.; Taranu, I. A comparison between the effects of ochratoxin A and aristolochic acid on the inflammation and oxidative stress in the liver and kidney of weanling piglets. *N-S Arch. Pharmacol.* **2018**, *391*, 1147–1156. [[CrossRef](#)]
11. Poon, S.L.; Pang, S.T.; McPherson, J.R.; Yu, W.; Huang, K.K.; Guan, P.; Weng, W.H.; Siew, E.Y.; Liu, Y.; Heng, H.L. Genome-Wide Mutational Signatures of Aristolochic Acid and Its Application as a Screening Tool. *Sci. Transl. Med.* **2013**, *5*, 197ra101. [[CrossRef](#)]
12. Ang, L.P.; Ng, P.W.; Lean, Y.L.; Kotra, V.; Kifli, N.; Goh, H.P.; Lee, K.S.; Ming, L.C. Herbal products containing aristolochic acids: A call to revisit the context of safety. *J. Herb. Med.* **2021**, *28*, 100447. [[CrossRef](#)]
13. van Montfoort, J.E.; Hagenbuch, B.; Groothuis, G.M.M.; Koepsell, H.; Meier, P.J.; Meijer, D.K.F. Drug uptake systems in liver and kidney. *Curr. Drug Metab.* **2003**, *4*, 185–211. [[CrossRef](#)]
14. Zhang, H.M.; Zhao, X.H.; Sun, Z.H.; Li, G.C.; Liu, G.C.; Sun, L.R.; Hou, J.Q.; Zhou, W. Recognition of the toxicity of aristolochic acid. *J. Clin. Pharm. Ther.* **2019**, *44*, 157–162. [[CrossRef](#)]
15. Xu, D.; Ran, C.L.; Yin, L.Z.; Lin, J.C.; Shu, G. Acute and Subchronic Toxicity Studies of Aristolochic Acid A in Tianfu Broilers. *Animals* **2021**, *11*, 1556. [[CrossRef](#)]
16. Draghia, L.P.; Lukinich-Gruia, A.T.; Oprean, C.; Pavlovic, N.M.; Tatu, C.A. Aristolochic acid I: An investigation into the role of food crops contamination, as a potential natural exposure pathway. *Environ. Geochem. Health* **2021**, *1*, 123. [[CrossRef](#)] [[PubMed](#)]
17. Lin, S.Y.; Xu, D.; Du, X.X.; Ran, C.L.; Shu, G. Protective Effects of Salidroside against Carbon Tetrachloride (CCl<sub>4</sub>)-Induced Liver Injury by Initiating Mitochondria to Resist Oxidative Stress in Mice. *Int. J. Mol. Sci.* **2019**, *20*, 3187. [[CrossRef](#)] [[PubMed](#)]
18. Li, T.; Na, R.; Yu, P.; Shi, B.; Yan, S. Effects of dietary supplementation of chitosan on immune and antioxidative function in beef cattle. *Czech. J. Anim. Sci.* **2015**, *60*, 38–44. [[CrossRef](#)]
19. Marin, D.E.; Braicu, C.; Gras, M.A.; Pistol, G.C.; Taranu, L. Low level of ochratoxin A affects genome-wide expression in kidney of pig. *Toxicol* **2017**, *136*, 67. [[CrossRef](#)]
20. Bunel, V.; Antoine, M.H.; Nortier, J.; Duez, P.; Stevigny, C. In Vitro Effects of Panax ginseng in Aristolochic Acid-Mediated Renal Tubulotoxicity: Apoptosis versus Regeneration. *Planta. Med.* **2015**, *81*, 363–372. [[CrossRef](#)]
21. Wu, T.K.; Pan, Y.R.; Wang, H.F.; Yu, Y.L. Vitamin E ( $\alpha$ -tocopherol) ameliorates aristolochic acid-induced renal tubular epithelial cell death by attenuating oxidative stress and caspase3 activation. *Mol. Med. Rep.* **2018**, *17*, 31–36.
22. Pesti, G.M. Nutrient requirements of poultry. *Anim. Feed. Sci. Tech.* **1995**, *56*, 177–178. [[CrossRef](#)]
23. Wang, Y.W.; Guo, Y.M.; Ning, D. Changes of hepatic biochemical parameters and proteomics in broilers with cold-induced ascites. *J. Anim. Sci. Biotechnol.* **2012**, *3*, 1–9. [[CrossRef](#)] [[PubMed](#)]
24. Uni, Z.; Gal-Garber, O.; Geyra, A.; Sklan, D.; Yahav, S. Changes in Growth and Function of Chick Small Intestine Epithelium Due to Early Thermal Conditioning. *Poult. Sci.* **2001**, *80*, 438–445. [[CrossRef](#)]
25. Thoolen, B.; Maronpot, R.R.; Takanori, H.; Abraham, N.; Colin, R.; Thomas, N.; Wolfgang, K.; Karin, K.; Ulrich, D.; Dai, N.; et al. Proliferative and Nonproliferative Lesions of the Rat and Mouse Hepatobiliary System. *Toxicol. Pathol.* **2010**, *38*, 5S–81S. [[CrossRef](#)]

26. Wang, F.Y.; Zuo, Z.C.; Chen, K.J.; Gao, C.X.; Yang, Z.Z.; Zhao, S.; Li, J.Z.; Song, H.T.; Peng, X.; Fang, J. Histopathological Injuries, Ultrastructural Changes, and Depressed TLR Expression in the Small Intestine of Broiler Chickens with Aflatoxin B1. *Toxins* **2018**, *10*, 131. [[CrossRef](#)]
27. Jian, Z.; Luxia, Z.; Wenke, W.; Haiyan, W. Association Between Aristolochic Acid and CKD: A Cross-sectional Survey in China—ScienceDirect. *Am. J. Kidney Dis.* **2013**, *61*, 918–922.
28. Cosyns, J.P.; Dehoux, J.P.; Guiot, Y.; Goebbels, R.M.; Cvyd, S. Chronic aristolochic acid toxicity in rabbits: A model of Chinese herbs nephropathy. *Kidney Int.* **2001**, *59*, 2164–2173. [[CrossRef](#)]
29. Mengs, U. Tumour induction in mice following exposure to aristolochic acid. *Arch. Toxicol.* **1988**, *61*, 504–505. [[CrossRef](#)] [[PubMed](#)]
30. Bellamri, M.; Brandt, K.; Brown, C.V.; Wu, M.T.; Turesky, R.J. Cytotoxicity and genotoxicity of the carcinogen aristolochic acid I (AA-I) in human bladder RT4 cells. *Arch. Toxicol.* **2021**, *95*, 1–11. [[CrossRef](#)]
31. Zhao, Q.Y.; Hou, D.Z.; Laraib, Y.; Xue, Y.; Shen, Q. Comparison of the effects of raw and cooked adzuki bean on glucose/lipid metabolism and liver function in diabetic mice. *Cereal Chem.* **2021**, *98*, 10456. [[CrossRef](#)]
32. Wang, X.; Xia, H.J.; Liu, Y.P.; Qiu, F.; Di, X. Simultaneous determination of three glucuronide conjugates of scutellarein in rat plasma by LC–MS/MS for pharmacokinetic study of breviscapine. *J. Chromatogr. B* **2014**, *965*, 79–84. [[CrossRef](#)]
33. Traesel, G.K.; Menegati, S.E.L.T.; Santos, A.C.D.; Boas, G.R.V.; Justi, P.N.; Kassuya, C.A.L.; Argandoa, E.J.S.; Oesterreich, S.A. Oral acute and subchronic toxicity studies of the oil extracted from pequi (*Caryocar brasiliense*, Camb.) pulp in rats. *Food Chem. Toxicol.* **2016**, *97*, 224–231. [[CrossRef](#)] [[PubMed](#)]
34. Sookoian, S.; Pirola, C. Liver enzymes, metabolomics and genome-wide association studies: From systems biology to the personalized medicine. *World. J. Gastroenterol.* **2015**, *21*, 711–725. [[CrossRef](#)]
35. Khattab, H.; Fouad, A.; Hamza, M.A.; Mohey, M.; El-Akel, W.; Ghoneim, H.; Abul-Fotouh, A.; Esmat, G. Relation of ALT and AST levels to the histopathological changes in liver biopsies of patients with chronic hepatitis C genotype 4. *Arab. J. Gastroenterol.* **2015**, *16*, 50–53. [[CrossRef](#)] [[PubMed](#)]
36. Yeh, Y.H.; Lee, Y.T.; Hsieh, H.S.; Hwang, D.F. Short-term toxicity of aristolochic acid, aristolochic acid-I and aristolochic acid-II in rats. *Food Chem. Toxicol.* **2008**, *46*, 1157–1163. [[CrossRef](#)] [[PubMed](#)]
37. Zhou, J.; Yang, Y.; Wang, H.; Bian, B.; Zhao, H. The Disturbance of Hepatic and Serous Lipids in Aristolochic Acid I Induced Rats for Hepatotoxicity Using Lipidomics Approach. *Molecules* **2019**, *24*, 3745. [[CrossRef](#)]
38. Schmeiser, H.H.; Frei, E.; Wiessler, M.; Stiborova, M. Comparison of DNA adduct formation by aristolochic acids in various in vitro activation systems by 32P-post-labelling: Evidence for reductive activation by peroxidases. *Carcinogenesis* **1997**, *18*, 1055–1062. [[CrossRef](#)]
39. Cabiscol, E.; Tamarit, J.; Ros, J. Oxidative stress in bacteria and protein damage by reactive oxygen species. *Int. Microbiol.* **2000**, *3*, 3–8.
40. Youl, E.; Husson, C.; El Khattabi, C.; El Mere, S.; Antoine, M.H. Characterization of cytotoxic effects of aristolochic acids on the vascular endothelium. *Toxicol. In Vitro* **2020**, *65*, 104811. [[CrossRef](#)]
41. Zhang, Y.; Shiyang, X.Y.; Li, Y.; Shi, X.; Xiong, B. Exposure to aristolochic acid I compromises the maturational competency of porcine oocytes via oxidative stress-induced DNA damage. *Aging-Us* **2019**, *11*, 2241–2252. [[CrossRef](#)] [[PubMed](#)]
42. Loboda, A.; Damulewicz, M.; Pyza, E.; Jozkowicz, A.; Dulak, J. Role of Nrf2/HO-1 system in development, oxidative stress response and diseases: An evolutionarily conserved mechanism. *Cell. Mol. Life Sci.* **2016**, *73*, 3221–3247. [[CrossRef](#)]
43. Li, L.R.; Dong, H.; Song, E.Q.; Xu, X.Y.; Liu, L.C.; Song, Y. Nrf2/ARE pathway activation, HO-1 and NQO1 induction by polychlorinated biphenyl quinone is associated with reactive oxygen species and PI3K/AKT signaling. *Chem.-Biol. Interact.* **2014**, *209*, 56–67. [[CrossRef](#)]
44. Shu, G.; Xu, D.; Ran, C.L.; Yin, L.Z.; Amevor, F.K. Protective effect of dietary supplementation of Bupleurum falcatum L saikosaponins on ammonia exposure induced ileum injury in broilers. *Poult. Sci.* **2020**, *100*, 100803. [[CrossRef](#)] [[PubMed](#)]
45. Romanov, V.; Whyard, T.C.; Waltzer, W.C.; Grollman, A.P.; Rosenquist, T. Aristolochic acid-induced apoptosis and G2 cell cycle arrest depends on ROS generation and MAP kinases activation. *Arch. Toxicol.* **2015**, *89*, 47–56. [[CrossRef](#)] [[PubMed](#)]
46. Guo, H.R.; Chen, L.; Cui, H.M.; Peng, X.; Wu, B.Y. Research Advances on Pathways of Nickel-Induced Apoptosis. *Int. J. Mol. Sci.* **2015**, *17*, 10. [[CrossRef](#)] [[PubMed](#)]
47. Guo, H.R.; Ouyang, Y.J.; Wang, J.Q.; Cui, H.M.; Tang, H.Q. Cu-induced spermatogenesis disease is related to oxidative stress-mediated germ cell apoptosis and DNA damage. *J. Hazard Mater.* **2021**, *416*, 125903. [[CrossRef](#)]
48. Zorov, B.D. Reactive Oxygen Species (ROS)-induced ROS Release: A New Phenomenon Accompanying Induction of the Mitochondrial Permeability Transition in Cardiac Myocytes. *J. Exp. Med.* **2000**, *192*, 1001–1014. [[CrossRef](#)]
49. Sinha, K.; Das, J.; Pal, P.B.; Sil, P.C. Oxidative stress: The mitochondria-dependent and mitochondria-independent pathways of apoptosis. *Arch. Toxicol.* **2013**, *87*, 1157–1180. [[CrossRef](#)] [[PubMed](#)]
50. Lee, J.; Giordano, S.; Zhang, J.H. Autophagy, mitochondria and oxidative stress: Cross-talk and redox signalling. *Biochem. J.* **2012**, *441*, 523–540. [[CrossRef](#)]
51. Liu, X.; Wu, J.; Wang, J.; Feng, X.; Yang, X. Mitochondrial dysfunction is involved in aristolochic acid I-induced apoptosis in renal proximal tubular epithelial cells. *Hum. Exp. Toxicol.* **2019**, *39*, 096032711989709. [[CrossRef](#)] [[PubMed](#)]